Journal of Pain Research

Dovepress
open access to scientific and medical research

Open Access Full Text Article

ORIGINAL RESEARCH

Pulsed Radiofrequency Decreases pERK and Affects Intracellular Ca^{2+} Influx, Cytosolic ATP Level, and Mitochondrial Membrane Potential in the Sensitized Dorsal Root Ganglion Neuron Induced by N-Methyl D-Aspartate

Ristiawan Muji Laksono[1,2], Handono Kalim[3], Mohammad Saifur Rohman[4], Nashi Widodo[5], Muhammad Ramli Ahmad[6], Willy Halim[7]

[1]Doctoral Program in Biomedical Science, Faculty of Medicine, Brawijaya University, Malang, Indonesia; [2]Department of Anesthesiology and Intensive Therapy, Faculty of Medicine, Brawijaya University, Malang, Indonesia; [3]Department of Internal Medicine, Faculty of Medicine, Brawijaya University, Malang, Indonesia; [4]Department of Cardiology and Vascular Medicine, Faculty of Medicine, Brawijaya University, Malang, Indonesia; [5]Department of Biology, Faculty of Mathematics and Natural Science, Brawijaya University, Malang, Indonesia; [6]Department of Anesthesiology, Intensive Care and Pain Management, Faculty of Medicine, Hasanuddin University, Makassar, Indonesia; [7]Faculty of Medicine, Brawijaya University, Malang, Indonesia

Correspondence: Ristiawan Muji Laksono, Department of Anesthesiology and Intensive Therapy, Faculty of Medicine, Brawijaya University, Jl. Jaksa Agung Suprapto No. 2, Malang, East Java, Indonesia, Tel +62 812-3377-3593, Email ristiawanm@ub.ac.id

Background: The molecular mechanism of pulsed radiofrequency (PRF) in chronic pain management is not fully understood. Chronic pain involves the activation of specific N-Methyl D-Aspartate receptors (NMDAR) to induce central sensitization. This study aims to determine the effect of PRF on central sensitization biomarker phosphorylated extracellular signal-regulated kinase (pERK), Ca^{2+} influx, cytosolic ATP level, and mitochondrial membrane potential ($\Delta\psi m$) of the sensitized dorsal root ganglion (DRG) neuron following NMDAR activation.

Methods: This study is a true experimental in-vitro study on a sensitized DRG neuron induced with 80 μM NMDA. There are six treatment groups including control, NMDA 80 μM, Ketamine 100 μM, PRF 2Hz, NMDA 80 μM + PRF 2 Hz, and NMDA 80 μM + PRF 2 Hz + ketamine 100 μM. We use PRF 2 Hz 20 ms for 360 seconds. Statistical analysis was performed using the One-Way ANOVA and the Pearson correlation test with α=5%.

Results: In the sensitized DRG neuron, there is a significant elevation of pERK. There is a strong correlation between Ca^{2+}, cytosolic ATP level, and $\Delta\psi m$ with pERK intensity ($p<0.05$). PRF treatment decreases pERK intensity from 108.48 ± 16.95 AU to 38.57 ± 5.20 AU ($p<0.05$). PRF exposure to sensitized neurons also exhibits a Ca^{2+} influx, but still lower than in the unexposed neuron. PRF exposure in sensitized neurons has a higher cytosolic ATP level (0.0458 ± 0.0010 mM) than in the unexposed sensitized neuron (0.0198 ± 0.0004 mM) ($p<0.05$). PRF also decreases $\Delta\psi m$ in the sensitized neuron from 109.24 ± 6.43 AU to 33.21 ± 1.769 AU ($p<0.05$).

Conclusion: PRF mechanisms related to DRG neuron sensitization are by decreasing pERK, altering Ca^{2+} influx, increasing cytosolic ATP level, and decreasing $\Delta\psi m$ which is associated with neuron sensitization following NMDAR activation.

Keywords: pulsed radiofrequency, neurons, sensitization, calcium, ATP, mitochondrial membrane potential, NMDA, NMDAR

Introduction

Chronic pain become one-third to one-half of the world's population problem, with an annual incidence of 8%, and affects 13–50% of the adult population.[1,2] The prevalence of chronic pain conditions was 37.3% in developed countries and 41.1% in developing countries.[3] Chronic pain is associated with the activation of the N-methyl-D-aspartate receptor (NMDAR), one of the glutamate receptors,[4] which also plays a role in synaptic plasticity,[5] central sensitization, and pain

Received: 23 February 2023
Accepted: 8 May 2023
Published: 22 May 2023

hypersensitivity.[6] NMDAR activation in neurons is mediated by the α-amino-3-hydroxy-5-methyl-4-isoxazole propionic acid (AMPAR) response which causes neuronal depolarization. Depolarization of neurons cause Mg^{2+} ions unblocked from NMDAR which facilitates ion influx.[5] NMDAR's activation activates downstream cascade reactions such as increased intracellular calcium influx which acts as a secondary messenger in mitogen-activated protein kinases (MAP kinase), one of the pain pathways. MAP activation resulting in the elevation of the phosphorylated extracellular signal-regulated kinase (pERK) which increases the translation of NMDAR and AMPAR and their expression in the cell membrane, leading to central sensitization. In addition, pERK also increases the transcription of several genes related to central sensitization.[7]

Central sensitization leads to chronic pain formation, characterized by hyperalgesia and allodynia.[8] Central sensitization involves enhancing neuron synaptic activity, and enlargement of the receptive field.[9] Sensitized neurons also experience more rapid neuron activity related to energy consumption and generation. Sensitized neurons consume a lot of energy which has implications for cell activity in energy generation.[10,11]

In chronic pain management, dorsal root ganglion (DRG) neurons become the preferred target therapy due to their function in chronic pain pathology. DRG neurons mainly construct primary sensory neurons which mediate pain perception.[12] DRG neuron axons also contain several types of fiber (Aβ, Aδ, and C fiber) which mediated chronic pain formation.[13] DRG also play role in ectopic firing associated with central sensitization in neuropathic pain. In chronic pain, DRG neurons become the source of pain signals after injury (both peripheral nerve injury or DRG injury) and transmit the signals to the central nervous system.[13,14]

Pulsed radiofrequency (PRF) is one of the pain interventions used due to its efficacy in reducing pain with minimal tissue damage and side effects compared to continuous radiofrequency (CRF).[15,16] PRF delivers short waves of radiofrequency (2 or 4 Hz) in the radiofrequency range of 500 kHz.[17] In clinical use, PRF reports effective in ameliorating various types of pain, including neck pain, trigeminal neuralgia, back pain, facet arthropathy, postoperative pain, radicular pain, hip pain, myofascial pain, and adhesive capsulitis.[17–19] Although it has been used in clinical applications, the mechanism of action of PRF in treating chronic pain has not been fully understood. Review report that PRF is thought to affect several biological pain pathways.[20] Some theories suggest that PRF ameliorates pain through the generation of the electric field which affects the membrane potential and function of neurons,[15] as well as cell organelles.[21]

Experimental studies to explain the mechanism of action of PRF in chronic pain reduction are limited. We hypothesize that PRF may affect DRG neuron sensitization following NMDAR activation. In the experimental study, NMDAR opening is in response to its binding to NMDA or glycine.[22] NMDA is the NMDAR agonist which could activate NMDAR by binding to the GluN2 subunit and demonstrate the information transmission to the cell following ligand receptor binding.[23] Therefore, we investigate the effect of PRF treatment on the sensitization of the sensitized DRG neuron as well as on intracellular Ca^{2+} influx, cytosolic ATP, and mitochondrial membrane potential ($\Delta\psi m$) associated with neuron sensitization.

Materials and Methods

Cell Culture

We use the immortalized DRG cell line F11 (08062601, Sigma, USA), first described by Platika et al.[24] The cell culture method refers to Hashemian et al[25] with modification. The F11 cell line was cultured in Ham F-12 medium, 10% Fetal Bovine Serum (FBS), HAT medium (5 mM sodium hypoxanthine, 20 μM aminopterin, and 0.8 mM thymidine), 100 U/mL penicillin and 100 μg/mL streptomycin. Cells were cultured in 25 cm^2 flasks in a cell culture incubator with 5% CO_2 at 37 °C. Subcultures were performed when cells reached 60–70% confluency. The F-11 cell-line differentiation method into dorsal root ganglion (DRG) was carried out based on Pastori et al[26] with modification. The assessment of differentiated DRG neurons derived from the F11 cell line was based on a morphological and biomolecular approach. Microtubule-associated protein 2 (MAP2) biomarker (GTX50810, GeneTex, USA) was used as a biomarker for the most optimum neuron differentiation. The assessment was done on days 0, 4, 5, 10, and 12 of cell culture. MAP2 measurement using five replications in each group.

Microtubule-Associated Protein 2 (MAP2) Measurement

Microtubule-associated protein 2 (MAP2) measurement was carried out using the immunocytochemistry approach to obtain the well-differentiated DRG neuron. The cell culture was fixed. The aspirated cell medium was then added 2–3 mm above the cell surface with 4% formaldehyde in 1x Phosphate buffer saline (PBS). Cells were fixed for 15 minutes at room temperature. The fixative was aspirated, then the cells were washed 3 times using 1 x PBS for 5 minutes each washing. The next stage is immunostaining. Cells were supplemented with 1x PBS blocking buffer / 5% normal serum / 0.3% Triton™ (X-100). Blocking buffer was aspirated, then Microtubule-associated protein 2 (MAP2) (GTX50810, GeneTex, USA) primary antibody was added at a 1:200 dilution in antibody dilution buffer (1x PBS / 1% BSA / 0.3% Triton) (X-100). Next, the cells were incubated overnight at 4°C. Cells were washed 3 times in 1x PBS for 5 min for each wash. Cells were incubated in goat anti-rabbit IgG secondary antibody FITC (31635, Thermo Fisher Scientific, USA) which had been diluted in antibody dilution buffer for 1–2 hours at room temperature in the dark. Cells were washed with 1x PBS 3 times for 5 minutes each wash. The cell was observed by fluorescent microscopy at the appropriate excitation wavelengths.

Validation of DRG Neuron Sensitization Following NMDAR Activation

Neuron sensitization was induced using N-Methyl D-Aspartate (NMDA). To validate neuron sensitization, we analyze the phosphorylated extracellular signal-regulated kinase (pERK) intensity in the neuron. ERK phosphorylation is downstream reaction of NMDAR activation and is known as a neuron sensitization biomarker. NMDAR opening is in response to its binding to NMDA or glycine,[22] therefore we induce the differentiated DRG with several NMDA concentrations (10, 20, 40, 60, 80, and 100 μM) to specifically activate NMDAR to induce DRG neuron sensitization. The optimum concentration of NMDA in elevating pERK will be used to induce the DRG neuron sensitization in the treatment groups.

Treatment Groups and Pulsed Radiofrequency (PRF) Treatment

There are six treatment groups with four replications each group. A sensitized neuron was induced by giving 80 μM NMDA to specifically activate NMDAR. Control receive no intervention, the second group receive NMDA 80 μM, third receive ketamine 100 μM, fourth receive PRF 2 Hz, fifth receive NMDA 80 μM followed by PRF 2 Hz, and the last receive NMDA 80 μM, PRF 2 Hz and ketamine 100 μM. Ketamine is used as an NMDAR blocker to determine the reversible effect of NMDAR activation. Pulsed radiofrequency was carried out immediately in the 80 μM NMDA + 2 Hz PRF and 80 μM NMDA + 2 Hz PRF + 100 μM ketamine group after NMDA administration. The PRF treatment was carried out using a Cosman RF generator (Cosman Medical Company, USA) by placing a 22-gauge SMK 54 mm, 5-mm active tip needle into the cell culture. Pulsed radiofrequency was performed using 500 kHz energy, pulse frequency of 2 Hz 20 ms, for 360 seconds.[27] The distance between the cell and the needle tip was 500–1000 μm (Figure 1). In this study, there are four measurements including pERK, intracellular Ca^{2+} influx, cytosolic ATP, and mitochondrial membrane potential ($\Delta\psi m$) measurement.

Phosphorylated Extracellular Signal-Regulated Kinase (pERK) Intensity Measurement

Measurement of pERK using the immunocytochemistry approach. The differentiated DRG neuron receives treatment according to treatment groups. The treated neurons were fixed. The aspirated cell medium was then added 2–3 mm above the cell surface with 4% formaldehyde in 1x phosphate buffer saline (PBS). Cells were fixed for 15 minutes at room temperature. The fixative was aspirated, then the cells were washed 3 times using 1 x PBS for 5 minutes each washing. The next stage is immunostaining. Cells were supplemented with 1x PBS blocking buffer / 5% normal serum / 0.3% Triton™ (X-100). Blocking buffer was aspirated, then polyclonal antibody Phospho (Erk1/2) Thr202/Tyr204 (36–8800, Thermo Fisher Scientific, USA) primary antibody was added at a 1:200 dilution in antibody dilution buffer (1x PBS / 1% BSA / 0.3% Triton) (X-100). Next, the cells were incubated overnight at 4°C. Cells were washed 3 times in 1x PBS for 5 min for each wash. Cells were incubated in goat anti-rabbit IgG secondary antibody FITC (31635, Thermo Fisher Scientific, USA) which had been diluted in antibody dilution buffer for 1–2 hours at room temperature in the dark. Cells

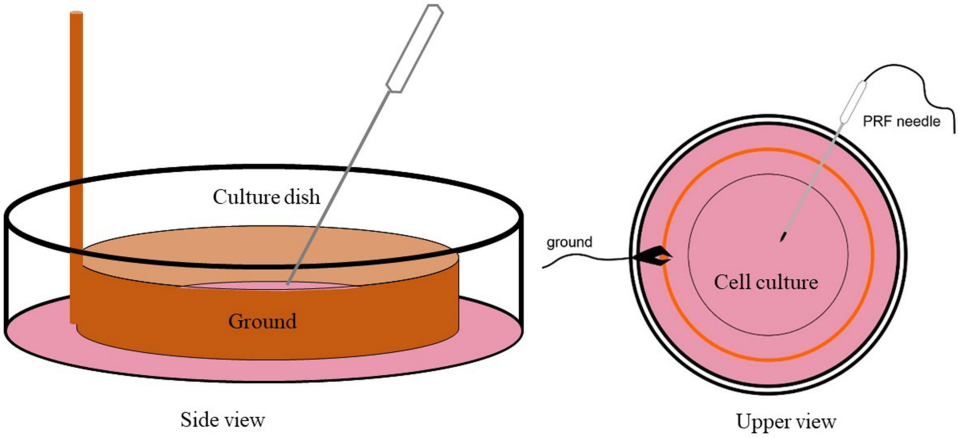

Figure 1 PRF treatment schematic in the neuron culture. Orange: PRF ground, pink: neuron culture.

were washed with 1x PBS 3 times for 5 minutes each wash. The cell was observed by fluorescent microscopy at the appropriate excitation wavelengths.

Intracellular Ca^{2+} Measurement

Measurement of intracellular calcium based on Pan et al[28] with modifications. Measurement of intracellular calcium ions was carried out simultaneously with the treatment while being observed under a microscope. Neurons were cultured on 24-well polystyrene tissue culture microtiter plates which had been coated with gelatin with a density of 1×10^6 cells/mL. Cells were cultured with 1 mL of media per well and incubated at 5% CO_2, 37 °C. Cells were added with 5×10−6 M Fluo-3/AM (F4897-1MG, Sigma-Aldrich, USA) in Dulbecco's modified eagle medium (DMEM) for 1 hour at room temperature and dark conditions. After that, the cells were washed, then the cells were immersed in PBS (without calcium) to measure the cytosolic calcium ion concentration. Calcium was observed using a confocal laser scanning microscope (CLSM) for 1 minute to determine the baseline calcium intensity. Then, the cells were given treatments according to groups. After treatment, the neuron cells were observed again using CLSM for 8 minutes to measure the intensity of intracellular calcium. Cells were observed at a wavelength of 340 and 380 nm. Filtered luminescence images (515 ± 25 nm) were taken.

Cytosolic ATP Level Measurement

ATP was measured using the ATP Assay Kit (Colorimetric/Fluorometric) (ab83355, Abcam, USA). Before measurement, the standard curve was made by diluting 10 µL standard ATP (stock concentration 10 mM) with 90 µL ddH_2O (final concentration 1 mM). The standard curve was made based on the following dilution table (Table 1).

The differentiated DRG neuron received treatment according to treatment groups. After that, the treated cells were incubated for 24 hours with 5% CO_2 at 37 °C for intracellular ATP measurement. A total of 1×10^6 cells were harvested and used for analysis. Cells were washed with PBS. Cells were resuspended in 100 µL ATP Assay Buffer. Cells were homogenized. Cells were centrifuged for 5 minutes at 4 °C and a speed of 13,000 g. The supernatant was put into a new tube and stored on ice. The cells were then deproteinated to prevent enzyme contamination. Cold 4 M perchloric acid (PCA) was added to the homogenate until the solution had a final concentration of 1 M, then homogenized. Samples were incubated for 5 minutes on ice. The sample was centrifuged for 2 minutes at 13,000 g (10,000 rpm) at 4 °C and the supernatant was transferred to a new tube. The supernatant volume was measured. Excess PCA is precipitated by adding 2 M cold KOH which is equivalent to 20–35% of the sample volume (sample + PCA). This neutralization process is carried out by adjusting the pH using 0.1 M KOH or PCA with a pH ranging from 6.5 to 8.0. Samples were centrifuged at 13,000 g for 15 minutes at 4 °C, then the supernatant was taken. This sample then used for measuring deproteinization dilution factor (DDF), using the following formula:

Table 1 Dilution Table for ATP Standard Curve Measurement

Standard	Standard ATP 1 mM (µL)	Buffer (µL)	Total Volume in Each Well (µL)	Total Amount of ATP Each Well (nmol/Well)
1	0	150	50	0
2	6	144	50	2
3	12	138	50	4
4	18	132	50	6
5	24	126	50	8
6	30	120	50	10

$$\mathrm{DF} = \frac{\text{Initial volume} + \text{volume PCA} + \text{volume KOH}(\mu\mathrm{L})}{\text{Initial volume in PCA}}$$

A total of 50 µL ATP reaction mix and background control mix for each group were prepared. A 50 µL of the reaction mix was added to each well of the 96-well plate containing the standard and sample. A 50 µL of background reaction mix was added to the background control sample well. Samples were homogenized and incubated at room temperature for 30 minutes in the dark. Samples were measured using a microplate reader at 570 nm. The amount of intracellular ATP is measured using the equation:

$$\text{ATP Concentration} = \left(\frac{B}{V} \times D\right) \times DDF$$

B: the amount of ATP in the sample calculated based on the standard curve
V: volume of sample added in well
D: sample dilution factor (if dilution is carried out to adjust within the measurement range)
DDF: deproteinization dilution factor

Mitochondrial Membrane Potential (Δψm) Measurement

The differentiated DRG neuron received treatment according to treatment groups. The mitochondrial staining method based on Pendergrass et al.[29] The treated cells were incubated for 24 hours with 5% CO_2 at 37 °C for mitochondrial membrane potential measurement. Treated cells were harvested by trypsinization and washed 2 times in PBS. Cells were resuspended in DMEM supplemented with 10% FBS, 25 mM DMEM medium, and stained with 40 nM MitoTrackerTM Green FM (M7514, Thermo Fisher Scientific, USA) for 30 min, at 37 °C. The cell was then washed with DMEM containing 10% FBS at 37 °C. The staining luminescence was observed using CLSM with excitation at 579 nm.

Statistical Analysis

The effect of PRF on pERK (neuron sensitization), cytosolic ATP level, and Δψm were analyzed using the One-Way ANOVA test with the Duncan Post Hoc test. Intracellular Ca^{2+} data is displayed descriptively to provide real-time Ca^{2+} fluctuation. The relationship between intracellular Ca^{2+}, cytosolic ATP level, and Δψm with neuronal sensitization (pERK) was analyzed using the Pearson Correlation test. Data analysis used statistical software SPSS 20.0 (IBM Statistics, USA) with α= 5% and 95% confidence interval.

Results

Sensitized DRG Neuron Following NMDA Induction

We use differentiated DRG neuron culture on day 5 which shows the optimum concentration of MAP2 expression (Figure 2A and Figure 2B) and differentiated neuron morphology (Figure 3). By using the different concentrations of NMDA, we found that NMDA 80 µM significantly has the highest pERK intensity (211.21 ± 0.37 AU) compared to

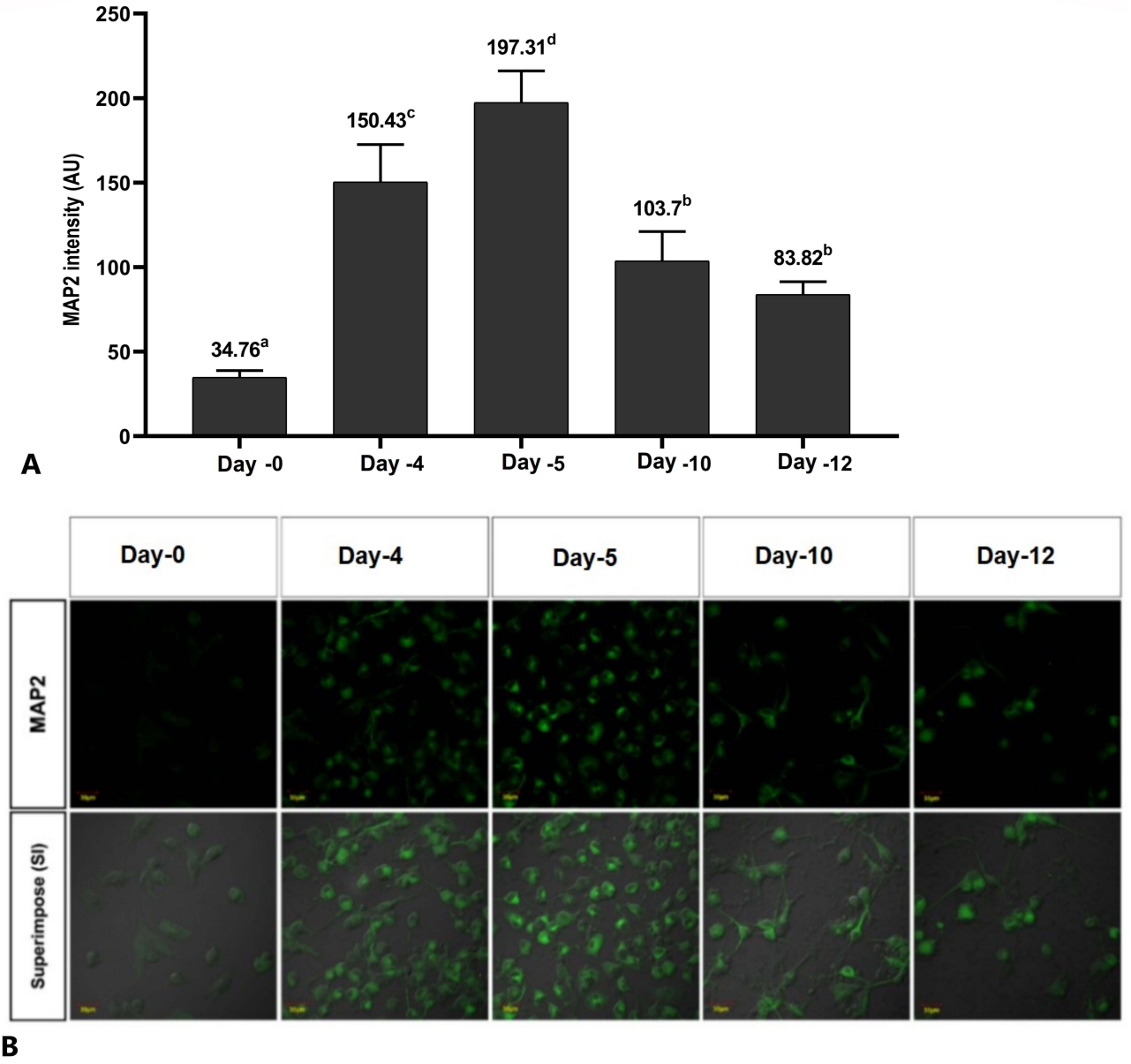

Figure 2 MAP2 intensity on the cell culture. (**A**) Cell culture on day 5 shows the highest MAP2 expression compared to other groups, (**B**) fluorescent imaging shows the highest MAP2 intensity on day 5. The [abcd] notation indicates statistical differences between groups. The same notation indicates no significant difference. Description: Superimpose (SI): description of the combined observations of MAP2 and DIC (differential interference contrast) observations. Magnification: 400X.

other groups ($p<0.05$), indicates the optimum sensitization (Figure 4). The NMDA 100 μM has the lowest pERK (2.31 ± 0.07 AU) compared to other groups. Based on this result, we use NMDA 80 μM to induce sensitization in the neuron.

PRF Decreased the pERK of the Sensitized DRG Neuron

This study report that the sensitized DRG neuron (NMDA 80 μM group) significantly had the highest pERK (108.48 ± 16.95 AU) compared to the control (42.11 ± 5.97 AU) and the other groups ($p <0.05$) (Figure 5A), also show by the highest green fluorescent (Figure 5B). PRF exposure to the sensitized DRG neurons (NMDA 80 μM + PRF 2Hz group) significantly had a lower pERK (38.57 ± 5.20 AU) than the sensitized DRG neuron. PRF exposure in the sensitized DRG neuron decrease pERK close to control/normal condition. Ketamine administration as an NMDAR blocker had a lower pERK (20.89 ± 3.03 AU) than the control and other groups.

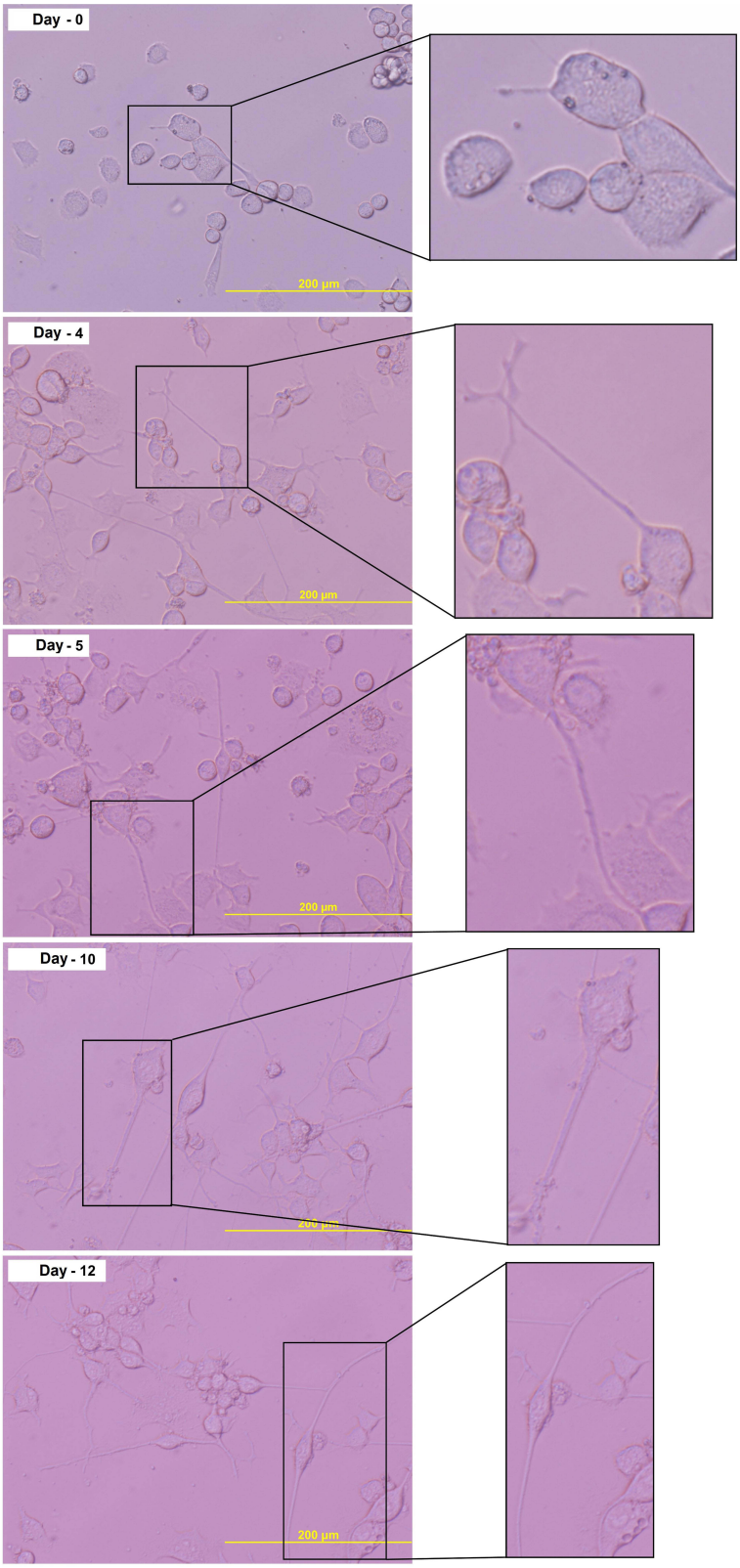

Figure 3 Morphological examination of the F11 cell line differentiation. Cell culture on day 5 shows the complete morphological features of the neuron.

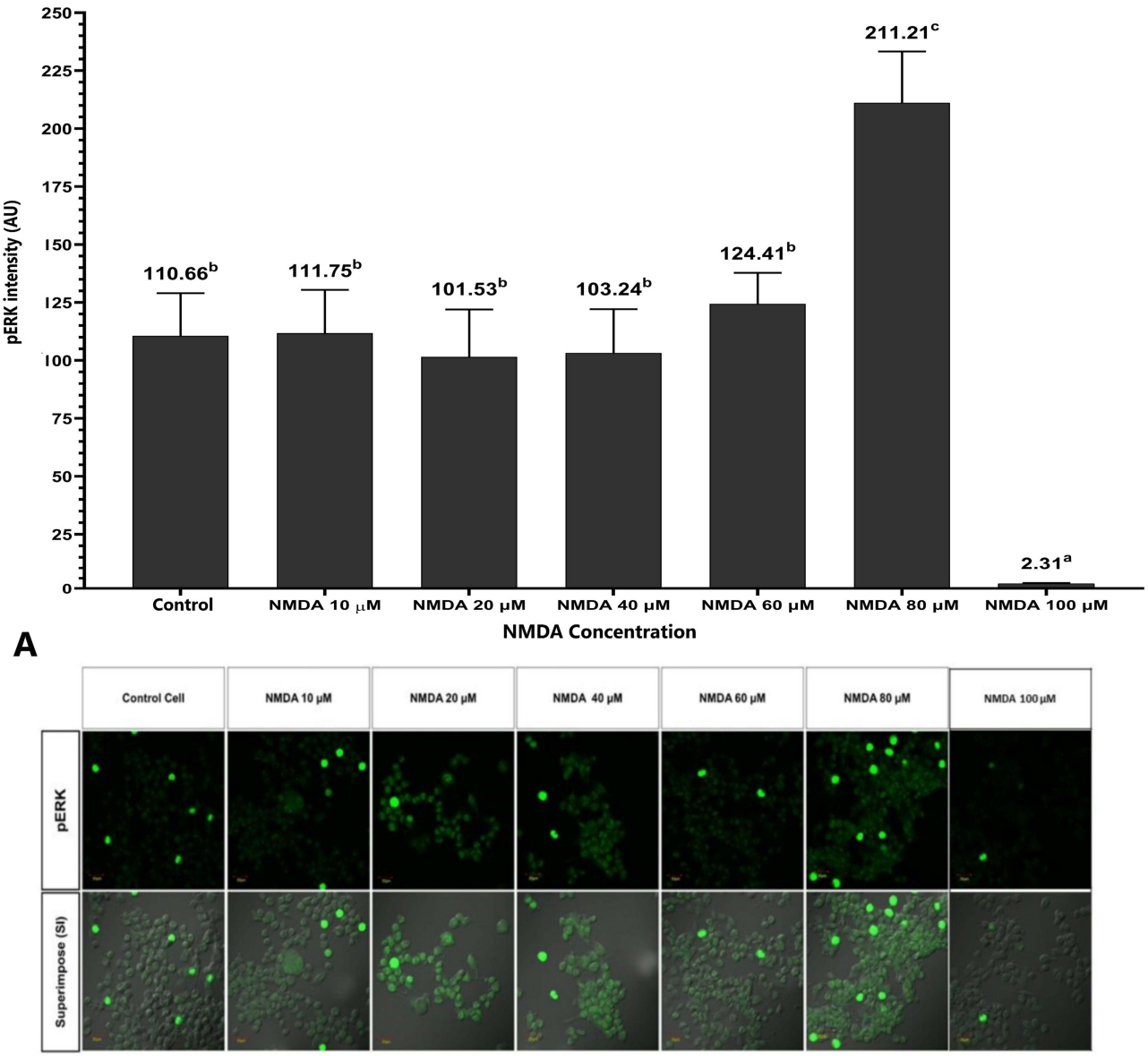

Figure 4 pERK intensity in the DRG neuron induced with a different concentration of NMDA . (**A**) Induction with NMDA 80 μM shows the highest pERK intensity compared to other groups. (**B**) Fluorescent imaging shows the highest intensity of pERK in the neuron induced with NMDA 80 μM. The ^{abc} notation indicates statistical differences between groups. The same notation indicate no significant difference. Description: Superimpose (SI): description of the combined observations of pERK and DIC (differential interference contrast) observations. Magnification: 400X.

Administration of ketamine to sensitized cells exposed to PRF had significant higher pERK (51.52 ± 733 AU) than neuronal cells treated only with ketamine, but not significantly different from sensitized DRG neurons exposed to PRF.

PRF Decreased Intracellular Calcium Influx in Sensitized DRG Neurons

The effect of PRF on intracellular Ca^{2+} influx is displayed in a descriptive graph. The sensitized DRG neuron induced by NMDA 80 μM experienced a significant calcium influx in the initial time of observation compared to the basal level (orange line). PRF exposure to sensitized DRG neurons also showed an increase in intracellular Ca^{2+} influx. However, the elevation is still lower than in unexposed sensitized neurons (blue line). Ketamine administration showed a decrease in intracellular calcium in the first

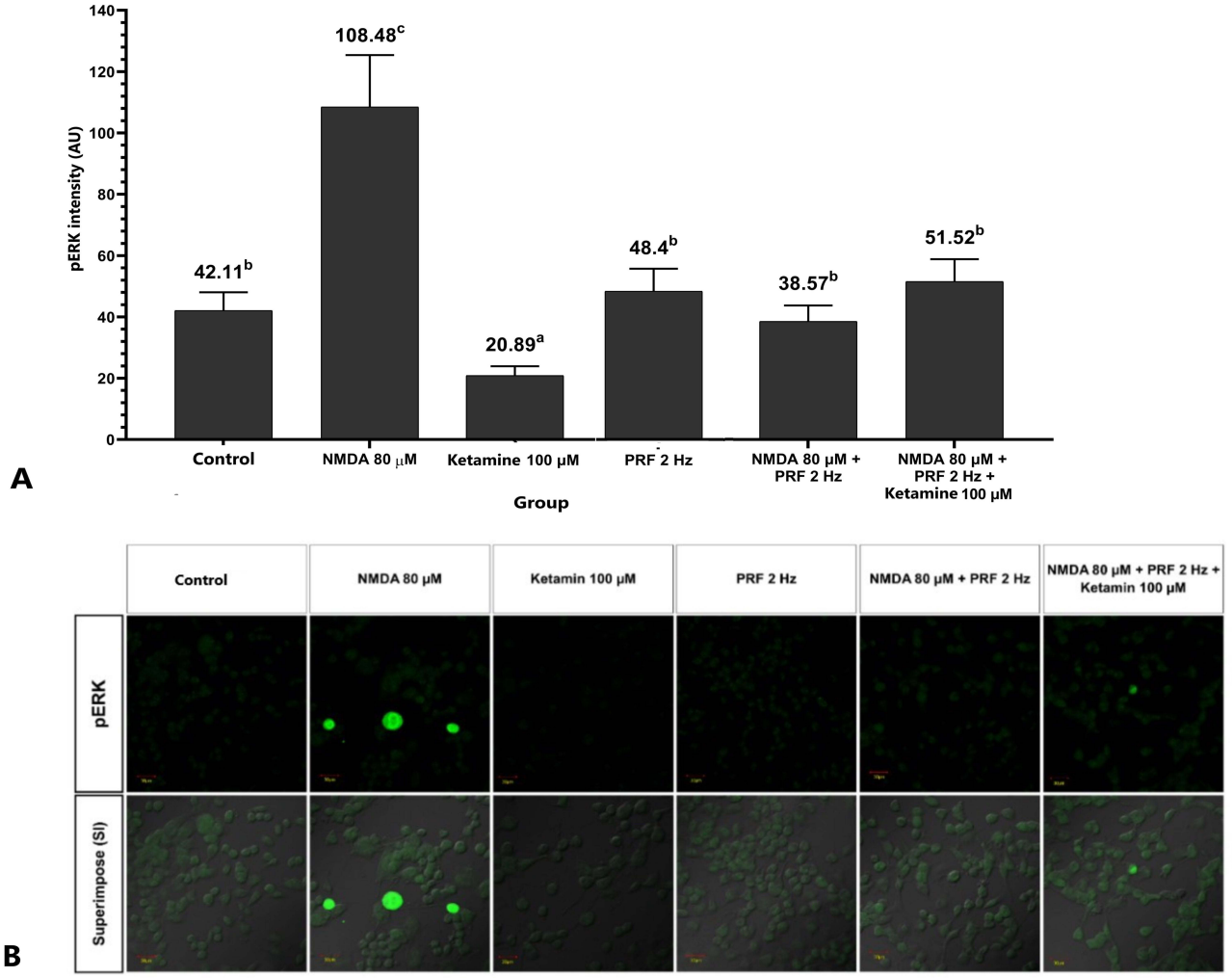

Figure 5 PRF decreases neuron sensitization in the sensitized DRG neuron. (**A**) Sensitized neurons significantly had a higher pERK than the control and other groups. PRF exposure to sensitized cells had a lower pERK intensity than unexposed neurons. (**B**) Fluorescent imaging show pERK expression. The ^{abc} notation indicates statistical differences between groups. The same notation indicate no significant difference. Description: Superimpose (SI): description of the combined observations of pERK and DIC (differential interference contrast) observations. Magnification: 400X.

seconds of observation compared to the basal level (orange line). Administration of ketamine to sensitized neurons exposed to PRF showed a significant decrease in intracellular calcium intensity compared to the basal level (violet line). Control group showed a stable Ca^{2+} during observation (Figure 6A and Figure 6B).

PRF Increases Cytosolic ATP Level in the Sensitized DRG Neuron

The sensitized DRG neuron (NMDA 80 μM group) had a significant lower cytosolic ATP level (0.0198 ± 0.0004 mM) than the control (0.0228 ± 0.0004 mM) and another treatment group ($p<0.05$). In sensitized neurons exposed to PRF (NMDA 80 μM+ PRF 2 Hz group), cytosolic ATP level was significantly higher (0.0458 ± 0.0010 mM) than in unexposed neurons. Administration of ketamine as an NMDAR blocker showed higher cytosolic ATP concentrations than controls. Administration of ketamine to sensitized neurons exposed to PRF had lower cytosolic ATP level than the neurons treated only with ketamine (Figure 7).

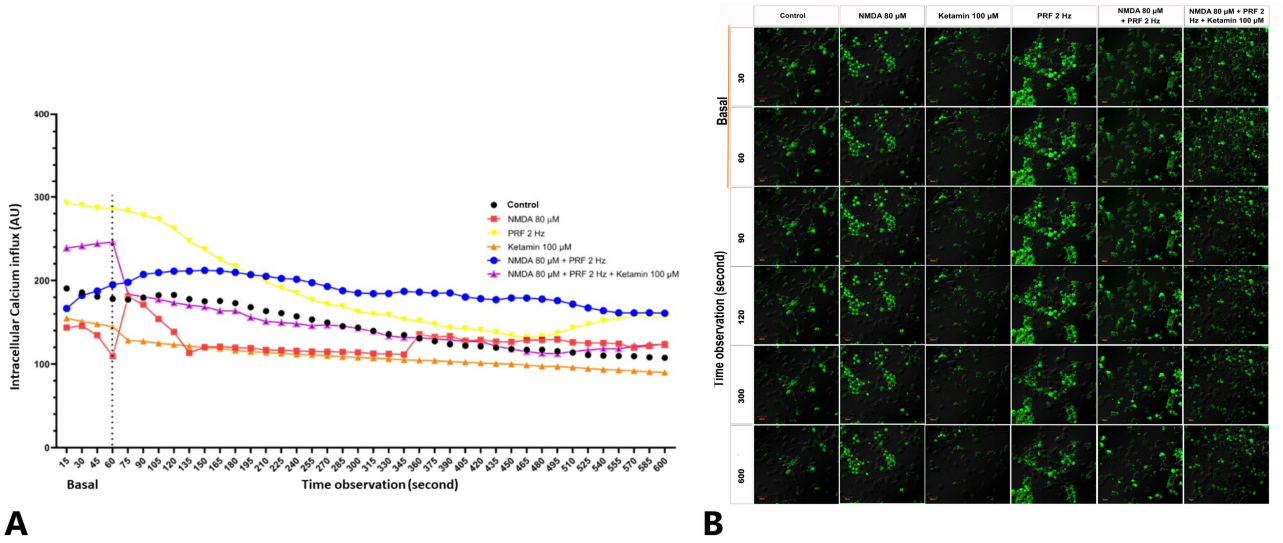

Figure 6 PRF decreases intracellular Ca^{2+} intensity in sensitized DRG neurons. (**A**) Sensitized neuronal experienced a significant increase in intracellular Ca^{2+} intensity at the initial time of observation compared to basal level (red). In sensitized neurons exposed to PRF, there was an increase in intracellular Ca^{2+} intensity, but not significantly compared to basal intensity (blue). (**B**) Fluorescent imaging show intracellular Ca^{2+} influx in basal and treatment. Description: Superimpose (SI): description of the combined observations of intracellular calcium and DIC (differential interference contrast) observations. Magnification: 400X.

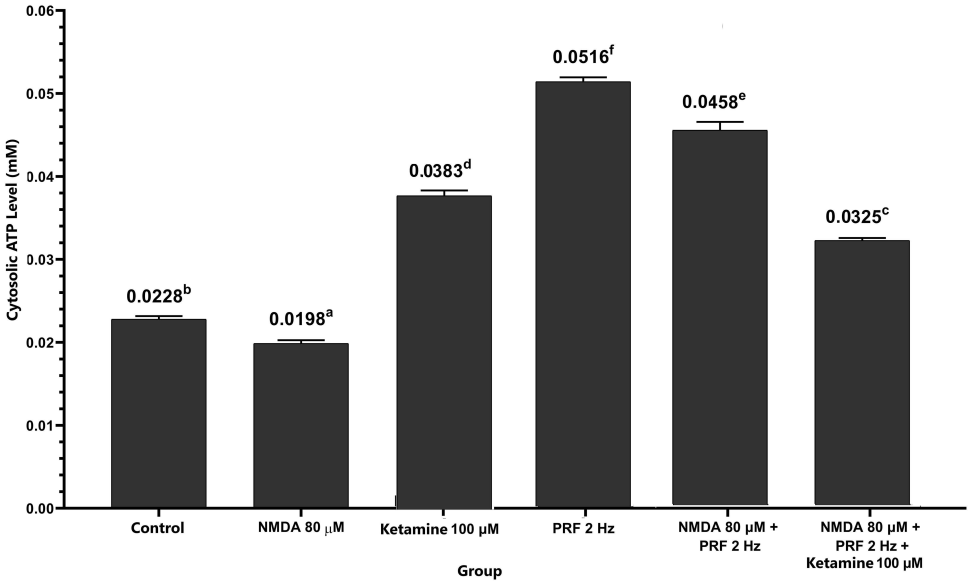

Figure 7 PRF causes an increase in cytosolic ATP in sensitized DRG neuron cells. Sensitized neuronal cells had significantly lower cytosolic ATP concentrations than controls. Sensitized neuronal cells exposed to PRF had significantly higher concentrations of cytosolic ATP than unexposed cells . The ^{abcdef} notation indicates statistical differences between groups. The same notation indicates no significant difference.

PRF Decreased Mitochondrial Membrane Potential (Δψm) in Sensitized DRG Neurons

The sensitized DRG neurons (NMDA 80 µM group) significantly had the highest mitochondrial membrane potential (Δψm) (109.24 ± 6.43 AU) compared to the control group (76.19 ± 5.09 AU) and other treatments ($p<0.05$). PRF exposure in sensitized neurons had significant lower Δψm (33.21 ±1.769 AU) than in unexposed neurons. Administration of ketamine as an NMDAR blocker showed lower Δψm intensity than controls. Administration of ketamine to sensitized neurons exposed to PRF shows no difference from the ketamine group (Figure 8A and Figure 8B).

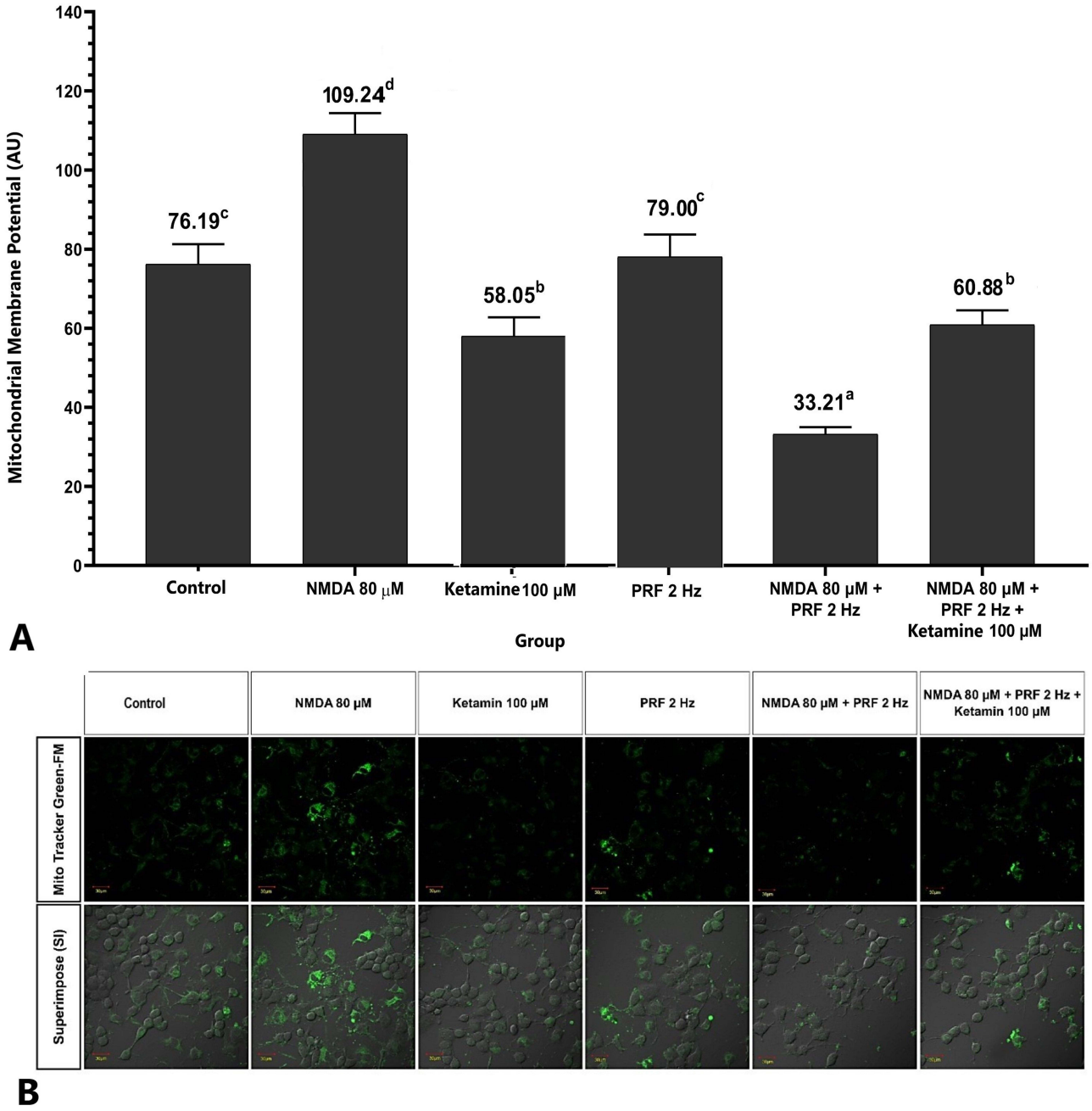

Figure 8 PRF decreases mitochondrial membrane potential (Δψm) in sensitized DRG neurons. (**A**) Sensitized neuron had the highest Δψm compared to the other groups. Sensitized neurons exposed to PRF had lower Δψm intensity than unexposed neurons. (**B**) Fluorescent imaging show lower Δψm intensity. The ^{abcd} notation indicates statistical differences between groups. Description: Superimpose (SI): description of the combined observations of Δψm and DIC (differential interference contrast) observations. Magnification: 400X.

Intracellular Ca^{2+} Influx, Cytosolic ATP, and Δψm Association with Neuron Sensitization

To analyze whether intracellular calcium intensity, cytosolic ATP, and Δψm are associated with the sensitization of the sensitized neuron, we perform a Pearson correlation test. Neuron sensitization represents by pERK. Intracellular Ca^{2+}, cytosolic ATP, and Δψm have a strong correlation with neuron sensitization ($p<0.05$). There is a strong positive correlation between intracellular Ca^{2+} and Δψm with pERK. However, there is a negative strong correlation between cytosolic ATP and pERK (Table 2).

Table 2 Correlation Test Between Intracellular Calcium, Δψm, and Cytosolic ATP Level on Sensitization of Sensitized Neuron

Neuronal Parameter (Mean ± SD)		pERK Level in Sensitized Neuron (Mean ± SD)	Pearson Correlation	
			p-value	R
Calcium influx	141.643± 25.31	108.48 ± 16.95	0.045	0.955
ΔΨM	99.806 ± 11.83		0.026	0.974
Cytosolic ATP level	0.0199± 0.0004		0.048	−0.952

Notes: R: correlation coefficient; ΔΨM: Mitochondrial membrane potential, significance if p<0.05.

Discussion

We use differentiated DRG neurons on day 5 derived from cell-line F11, first described by Platika et al.[24] Differentiated F11 cell line express action potential similar to DRG sensory neurons, and express large ion channels such as Ca^{2+} and Na^{+}.[30] This cell line also has been used for in vitro study evolving nociceptive sensory neuron. Differentiated cell-line F11 also expresses NMDAR which is essential in this study.[31] DRG derived from F11 also shows representative properties of DRG cells which are used in many studies involving neuropathic pain.[32,33]

In this study, DRG neurons exposed to 80 μM NMDA show the highest pERK intensity compared to other groups, indicating sensitization occurs. This study is in accordance with the previous study found that sensitized neurons experienced a significant elevation in pERK.[23] Administration of ketamine as an NMDAR blocker also showed the lowest pERK intensity compared to the other groups, showing no sensitization. Sensitized neurons are defined as increased primary sensory response and central synapses become hypersensitive to nociceptive stimuli thus underlying the formation of chronic pain.[34] The formation of chronic pain is mediated by the activation of specific NMDAR receptors which mediate the chronic pain cascade reaction, one of them by leading the pERK activation.[7] Phosphorylated ERK will be translocated to the nucleus to activate several transcription factors cAMP-response element-binding protein (CREB), which plays a role in the transcription of genes that trigger long-term neural plasticity.[7] The activation or ERK phosphorylation is known as a neuron sensitization biomarker.[23] NMDAR opening is in response to its binding to NMDA or glycine.[22]

Pulsed radiofrequency (PRF) is starting to be used in chronic pain management due to its ability to ameliorate pain without tissue and nerve damage.[21] Several clinical studies have shown successful pain management using PRF therapy.[35–40] Even though clinically proven, the mechanism of PRF therapy in chronic pain is not fully understood. Cellular and molecular studies that explain the PRF mechanism in reducing pain are limited. To determine the effect of PRF on reducing chronic pain, neuron sensitization becomes one of the important parameters to be analyzed. In this study, PRF exposure to the sensitized DRG neurons significantly decreases pERK. Decreased pERK is associated with reduced neuronal sensitization.[23] This study supports the previous study whereby PRF can inhibit synaptic activity.[27,41] We propose that decrease sensitization is one of the mechanisms involved. There are two in-vivo studies report a decrease in pERK in the spinal cord of animals with nerve injury after PRF administration. Lin et al[42] and Xu et al[43] found a decrease in pERK in the spinal cord in after 3 and 14 days after PRF therapy. In addition, pERK also induce long-term potentiation related to chronic pain by triggering AMPAR and NMDAR exocytosis.[7,44] Decreased pERK due to PRF may contribute to the inhibition of long-term potentiation. However, more study is needed to analyze this issue. As far as the author's knowledge, this is the first in-vitro study of the PRF effect in neuron sensitization of the NMDA-induced DRG neuron. This study reports an insight of PRF treatment mechanism by reducing DRG neuron sensitization following NMDAR activation.

Besides induce neuron sensitization, NMDAR activation also activates downstream cascade reaction and affect neuronal energy generation. To analyze the effect of PRF in the downstream cascade reaction of NMDAR, we also analyze the intracellular Ca^{2+} influx after PRF exposure. In chronic pain, NMDAR activation is followed by increased Ca^{2+} influx, a secondary messenger of mitogen-activated protein kinase (MAPK) pathway.[45] Ca^{2+} initiate the activation of protein kinase C (PKC), Src, Raf-1, MAPK/ERK kinase (MEK), and pERK cascade reactions which underlying chronic pain formation.[7] In the sensitized DRG neuron, there is a significant intracellular Ca^{2+} influx at the initial time of observation. In this study, PRF exposure to sensitized DRG neuron also caused Ca^{2+} influx. However, the elevation is lower than in unexposed sensitized

neurons. One recent study showed that PRF administered to kidney cells caused an increase in Ca^{2+} influx caused by mild electroporation. The increased Ca^{2+} influx is thought to be related to voltage gate channels.[46] The difference of Ca^{2+} influx in unexposed and exposed sensitized DRG neuron to PRF shows the possible mechanism of PRF. PRF works by altering Ca^{2+} influx following NMDAR activation. Moreover, we found a positive strong correlation between Ca^{2+} intensity and pERK, which show a linear correlation between Ca^{2+} influx and neuron sensitization.

In addition, this study also analyzed the effect of PRF on neuronal activity in energy generation related to neuron sensitization. Therefore, an analysis of cytosolic ATP levels and mitochondrial membrane potential of sensitized DRG neurons exposed to PRF. The sensitized DRG neuron significantly had lower cytosolic ATP levels than other groups. This is in accordance with the theory that activated neurons experience a decrease in ATP levels in the axons, which is thought to be due to increased ATP consumption.[11] This result is also supported by the negative correlation between cytosolic ATP levels and pERK, show a low cytosolic ATP levels in the sensitized neuron. Neuronal activity, especially synaptic activity, consumes at least 50% of ATP for reversal ion fluxes via postsynaptic receptors.[47] This condition is compensated by increased energy production to fulfil energy supply-demand. In sensitized neurons exposed to PRF, the cytosolic ATP concentration is significantly higher compared to the unexposed neurons. We assume that this high level of cytosolic ATP is the accumulation ATP during neuron sensitization. During sensitization, neuron produces high amount of ATP due to high energy demand. This may result in the accumulation of cytosolic ATP. In sensitized neuron, there is a significant increase in ERK phosphorylation, thus it is acceptable that there is a high ATP demand. Decrease neuron sensitization after PRF treatment, which reduce energy demand, then response by ATP-fine tuning mechanism to restore ATP back to homeostasis concentration.[47] One of the ATP fine-tuning mechanisms in activated neurons is related to the cytosolic calcium concentration.[48] Calcium is an ion that is important in mitochondrial activity in energy synthesis (ATP).[48,49] Neurons have a lower threshold for calcium influx than non-neuronal cells, making the cytosolic calcium concentration important in the regulation of ATP levels.[50] PRF exposure to sensitized neurons causes an increase in intracellular calcium influx, but not as high as in the sensitized state. It is also a possibility to cause of decreased ATP production.

The effect of PRF on DRG neuron sensitization was also observed in mitochondrial membrane potential ($\Delta\psi m$) since it related to ATP production[51,52] and may indicate mitochondrial activity in energy resistance. In the sensitized DRG neuron, there was a significant increase in $\Delta\psi m$ indicating increased mitochondrial activity. In general, increase in $\Delta\psi m$ can lead to an increase in ATP production because a higher $\Delta\psi m$ promotes the flow of protons back into the mitochondrial matrix through ATP synthase.[53,54] This is in accordance with the ATP-level measurement in this study. Sensitized DRG neuron had the lowest cytosolic ATP and responses by increased ATP generation, show by increase $\Delta\psi m$. PRF exposure to sensitized neurons has a lower $\Delta\psi m$ than the sensitized state. This could be associated with a decrease in neuronal sensitization in PRF-treated sensitized neuron, proved by a positive correlation between $\Delta\Psi m$ and pERK. Reduced sensitization results in decreased ATP demand. Mitochondria responds to this condition by decreased $\Delta\Psi m$.

Studies reporting the molecular mechanism of PRF on molecular properties during pain are limited. Therefore, this finding should give an insight on PRF effect on neuron sensitization, Ca^{2+} influx, cytosolic ATP level, and $\Delta\Psi m$. In this study, we found a strong correlation between Ca^{2+} influx, cytosolic ATP level, and $\Delta\Psi m$ with pERK. PRF exposure to sensitized DRG neuron following NMDAR activation shows decreased sensitization, which also affects the downstream mechanism, Ca^{2+} influx, cytosolic ATP level, and $\Delta\Psi m$. PRF also affects mitochondrial activity such as increasing cytosolic ATP level and decrease $\Delta\Psi m$. Due to the wide range of chronic pain pathway, more studies are required to display the whole mechanism of PRF in pain pathway.

Conclusion

In sensitized DRG neurons following NMDAR activation, there is an increase in pERK intensity. In addition, there was a significant increase in the intracellular Ca^{2+} influx, decreased cytosolic ATP level, and increased $\Delta\Psi m$ which correlate with neuron sensitization. Our study demonstrates PRF could reduce pERK in the sensitized DRG neuron. This study shows that PRF exposure exhibit Ca^{2+} influx both in the exposed and unexposed neurons. However, unexposed neurons exhibit a more significant Ca^{2+} influx. PRF exposure also increases cytosolic ATP, which is thought to be the accumulation of the increased ATP generation during sensitization. PRF also causes a decrease in $\Delta\Psi m$ in response to the decreased neuronal pERK. This finding underlies the mechanism of PRF in alleviating pain by affecting important

physiological-pain related process in the sensitized DRG neuron. This study also supports the clinical use of PRF in pain therapy by providing the PRF working mechanism.

Ethical Statement

The study methods were approved by Brawijaya University Ethical Clearance Committee (No. 114-KEP-UB-2020).

Disclosure

The authors report no conflicts of interest in this work.

References

1. De SJB, Grossmann E, Perissinotti D, et al. Prevalence of chronic pain, treatments, perception, and interference on life activities: Brazilian population-based survey. *Pain Res Manag*. 2017;2017. doi:10.1155/2017/4643830
2. Goldberg DS, Mcgee SJ. Pain as a global public health priority. *BMC Public Health*. 2011;11(1):770. doi:10.1186/1471-2458-11-770
3. Tsang A, Von Korff M, Lee S, et al. Common chronic pain conditions in developed and developing countries: gender and age differences and comorbidity with depression-anxiety disorders. *J Pain*. 2008;9(10):883–891. doi:10.1016/j.jpain.2008.05.005
4. Zhou HY, Chen SR, Pan HL. Targeting N-methyl-D-aspartate receptors for treatment of neuropathic pain. *Expert Rev Clin Pharmacol*. 2011;4 (3):379–388. doi:10.1586/ecp.11.17
5. Laumet G, Chen SR, Pan HL. NMDA receptors and signaling in chronic neuropathic pain. *Receptors*. 2017;30:103–119. doi:10.1007/978-3-319-49795-2_6
6. Youn DH, Gerber G, Sather WA. Ionotropic glutamate receptors and voltage-gated Ca2+ channels in long-term potentiation of spinal dorsal horn synapses and pain hypersensitivity. *Neural Plast*. 2013;2013. doi:10.1155/2013/654257
7. Ji RR, Gureau IVRW, Malcangio M, Strichartz GR. MAP kinase and pain. *Brain Res Rev*. 2009;60(1):135–148. doi:10.1016/j.brainresrev.2008.12.011
8. Bazzari AH, Bazzari FH. Advances in targeting central sensitization and brain plasticity in chronic pain. *Egypt J Neurol Psychiatry Neurosurg*. 2022;58(1). doi:10.1186/s41983-022-00472-y
9. Latremoliere A, Woolf C. Central sensitization: a generator of pain hypersensitivity by central neural plasticity. *J Sci Food Agric*. 2009;10 (9):895–926. doi:10.1016/j.jpain.2009.06.012.Central
10. Shetty PK, Galeffi F, Turner DA. Cellular links between neuronal activity and energy homeostasis. *Front Pharmacol*. 2012;3:1–14. doi:10.3389/fphar.2012.00043
11. Natsubori A, Tsunematsu T, Karashima A, et al. Intracellular ATP levels in mouse cortical excitatory neurons varies with sleep–wake states. *Commun Biol*. 2020;3(1):1–5. doi:10.1038/s42003-020-01215-6
12. Berger AA, Liu Y, Possoit H, et al. Dorsal root ganglion (DRG) and chronic pain. *Anesthesiol Pain Med*. 2021;11(2):1–10. doi:10.5812/aapm.113020
13. Esposito MF, Malayil R, Hanes M, Deer T. Unique characteristics of the dorsal root ganglion as a target for neuromodulation. *Pain Med*. 2019;20: S23–S30. doi:10.1093/pm/pnz012
14. Liu CN, Wall PD, Ben-Dor E, Michaelis M, Amir R, Devor M. Tactile allodynia in the absence of C-fiber activation: altered firing properties of DRG neurons following spinal nerve injury. *Pain*. 2000;85(3):503–521. doi:10.1016/S0304-3959(00)00251-7
15. Cosman ER. A comment on the history of the pulsed radiofrequency technique for pain therapy [2]. *Anesthesiology*. 2005;103(6):1312. doi:10.1097/00000542-200512000-00028
16. Cho JH, Lee DG. Translocation of ampa receptors in the dorsal horn of the spinal cord corresponding to long-term depression following pulsed radiofrequency stimulation at the dorsal root ganglion. *Pain Med*. 2020;21(9):1913–1920. doi:10.1093/PM/PNZ307
17. Chua NHL, Vissers KC, Sluijter ME. Pulsed radiofrequency treatment in interventional pain management: mechanisms and potential indications - A review. *Acta Neurochir*. 2011;153(4):763–771. doi:10.1007/s00701-010-0881-5
18. Kwak SG, Lee DG, Chang MC. Effectiveness of pulsed radiofrequency treatment on cervical radicular pain A meta-analysis. *Medicine*. 2018;97 (31):1–6. doi:10.1097/MD.0000000000011761
19. Wu YT, Ho CW, Chen YL, Li TY, Lee KC, Chen LC. Ultrasound-guided pulsed radiofrequency stimulation of the suprascapular nerve for adhesive capsulitis: a prospective, randomized, controlled trial. *Anesth Analg*. 2014;119(3):686–692. doi:10.1213/ANE.0000000000000354
20. Sam J, Catapano M, Sahni S, Ma F, Abd-Elsayed A, Visnjevac O. Pulsed radiofrequency in interventional pain management: cellular and molecular mechanisms of action – an update and review. *Pain Physician*. 2021;24(8):525–532.
21. Erdine S, Bilir A, Cosman ER. Ultrastructural changes in axons following exposure to pulsed radiofrequency fields. *Pain Pract*. 2009;9 (6):407–417. doi:10.1111/j.1533-2500.2009.00317.x
22. Chang HR, Kuo CC. The activation gate and gating mechanism of the NMDA receptor. *J Neurosci*. 2008;28(7):1546–1556. doi:10.1523/JNEUROSCI.3485-07.2008
23. Gao Y-J, Ji -R-R. c-fos or pERK, which is a better marker for neuronal activation and central sensitization after noxious stimulation and tissue injury? *Open Pain J*. 2009;2(1):11–17. doi:10.2174/1876386300902010011
24. Platika D, Boulos MH, Baizer L, Fishman MC. Neuronal traits of clonal cell lines derived by fusion of dorsal root ganglia neurons with neuroblastoma cells. *Proc Natl Acad Sci U S A*. 1985;82(10):3499–3503. doi:10.1073/pnas.82.10.3499
25. Hashemian S, Alhouayek M, Fowler CJ. TLR4 receptor expression and function in F11 dorsal root ganglion × neuroblastoma hybrid cells. *Innate Immun*. 2017;23(8):687–696. doi:10.1177/1753425917732824
26. Pastori V, D'Aloia A, Blasa S, Lecchi M. Serum-deprived differentiated neuroblastoma F-11 cells express functional dorsal root ganglion neuron properties. *PeerJ*. 2019;2019(10):1–20. doi:10.7717/peerj.7951
27. Cahana A, Vutskits L, Muller D. Acute differential modulation of synaptic transmission and cell survival during exposure to pulsed and continuous radiofrequency energy. *J Pain*. 2003;4(4):197–202. doi:10.1016/S1526-5900(03)00554-6

28. Pan L, Zhang P, Hu F, et al. Hypotonic stress induces fast, reversible degradation of the vimentin cytoskeleton via intracellular calcium release. *Adv Sci*. 2019;6(18):1–8. doi:10.1002/advs.201900865
29. Pendergrass W, Wolf N, Pool M. Efficacy of MitoTracker GreenTM and CMXRosamine to measure changes in mitochondrial membrane potentials in living cells and tissues. *Cytom Part A*. 2004;61(2):162–169. doi:10.1002/cyto.a.20033
30. Haberberger RV, Barry C, Matusica D. Immortalized dorsal root ganglion neuron cell lines. *Front Cell Neurosci*. 2020;14. doi:10.3389/fncel.2020.00184
31. Yin K, Baillie GJ, Vetter I. Neuronal cell lines as dorsal root ganglion neurons: a transcriptomic comparison. *Mol Pain*. 2016;12:1–17. doi:10.1177/1744806916646111
32. Martínez AL, Brea J, Monroy X, Merlos M, Burgueño J, Loza MI. A new of sensorial neuron-like cells for HTS of novel analgesics for neuropathic pain. *SLAS Discov*. 2019;24(2):158–168. doi:10.1177/2472555218810323
33. Vetter I, Lewis RJ. Characterization of endogenous calcium responses in neuronal cell lines. *Biochem Pharmacol*. 2010;79(6):908–920. doi:10.1016/j.bcp.2009.10.020
34. Fabbretti E. P2X3 ATP, receptors and neuronal sensitization. *Front Cell Neurosci*. 2013;7:1–6. doi:10.3389/fncel.2013.00236
35. Van Zundert J, Lamé IE, De Louw A, et al. Percutaneous pulsed radiofrequency treatment of the cervical dorsal root ganglion in the treatment of chronic cervical pain syndromes: a clinical audit. *Neuromodulation*. 2003;6(1):6–14. doi:10.1046/j.1525-1403.2003.03001.x
36. Chao SC, Lee HT, Kao TH, et al. Percutaneous pulsed radiofrequency in the treatment of cervical and lumbar radicular pain. *Surg Neurol*. 2008;70(1):59–65. doi:10.1016/j.surneu.2007.05.046
37. Wang F, Zhou Q, Xiao L, et al. A randomized comparative study of pulsed radiofrequency treatment with or without selective nerve root block for chronic cervical radicular pain. *Pain Pract*. 2017;17(5):589–595. doi:10.1111/papr.12493
38. Vanneste T, Van Lantschoot A, Van Boxem K, Van Zundert J. Pulsed radiofrequency in chronic pain. *Curr Opin Anaesthesiol*. 2017;30(5):577–582. doi:10.1097/ACO.0000000000000502
39. Erdem Y, Sir E. The efficacy of ultrasound-guided pulsed radiofrequency of genicular nerves in the treatment of chronic knee pain due to severe degenerative disease or previous total knee arthroplasty. *Med Sci Monit*. 2019;25:1857–1863. doi:10.12659/MSM.915359
40. Napoli A, Alfieri G, Scipione R, Andrani F, Leonardi A, Catalano C. Pulsed radiofrequency for low-back pain and sciatica. *Expert Rev Med Devices*. 2020;17(2):83–86. doi:10.1080/17434440.2020.1719828
41. Cahana A, Van Zundert J, Macrea L, Van Kleef M, Sluijter M. Pulsed radiofrequency: current clinical and biological literature available. *Pain Med*. 2006;7(5):411–423. doi:10.1111/j.1526-4637.2006.00148.x
42. Lin ML, Lin WT, Huang RY, et al. Pulsed radiofrequency inhibited activation of spinal mitogen-activated protein kinases and ameliorated early neuropathic pain in rats. *Eur J Pain*. 2014;18(5):659–670. doi:10.1002/j.1532-2149.2013.00419.x
43. Xu X, Fu S, Shi X, Liu R. Microglial BDNF, PI3K, and p-ERK in the spinal cord are suppressed by pulsed radiofrequency on dorsal root ganglion to ease SNI-induced neuropathic pain in rats. *Pain Res Manag*. 2019;2019. doi:10.1155/2019/5948686
44. Bevilaqua LRM, Cammarota M. PERK, mTORC1 and eEF2 interplay during long term potentiation: an Editorial for 'Genetic removal of eIF2a kinase PERK in mice enables hippocampal L-LTP independent of mTORC1 activity' on page 133. *J Neurochem*. 2018;146(2):119–121. doi:10.1111/jnc.14485
45. Deng M, Chen S, Chen H, Luo Y, Dong Y, Pan H. Mitogen-activated protein kinase signaling mediates opioid- induced presynaptic NMDA receptor activation and analgesic tolerance. *J Neurochem*. 2019;148(2):275–290. doi:10.1111/jnc.14628.Mitogen-Activated
46. Mercadal B, Vicente R, Ivorra A. Pulsed radiofrequency for chronic pain: in vitro evidence of an electroporation mediated calcium uptake. *Bioelectrochemistry*. 2020;136:107624. doi:10.1016/j.bioelechem.2020.107624
47. Vergara RC, Jaramillo-Riveri S, Luarte A, et al. The energy homeostasis principle: neuronal energy regulation drives local network dynamics generating behavior. *Front Comput Neurosci*. 2019;13:1–18. doi:10.3389/fncom.2019.00049
48. Davis GW. Not fade away: mechanisms of neuronal ATP homeostasis. *Neuron*. 2020;105(4):591–593. doi:10.1016/j.neuron.2020.01.024
49. Baughman JM, Perocchi F, Girgis HS, et al. Integrative genomics identifies MCU as an essential component of the mitochondrial calcium uniporter. *Nature*. 2011;476(7360):341–345. doi:10.1038/nature10234
50. Ashrafi G, De J-SJ, Farrell RJ, Ryan TA. ensures metabolic flexibility of neurotransmission. *Neuron*. 2021;105(4):678–687. doi:10.1016/j.neuron.2019.11.020
51. Morais VA, Verstreken P, Roethig A, et al. Parkinson's disease mutations in PINK1 result in decreased Complex I activity and deficient synaptic function. *EMBO Mol Med*. 2009;1(2):99–111. doi:10.1002/emmm.200900006
52. Wang HL, Chou AH, Wu AS, et al. PARK6 PINK1 mutants are defective in maintaining mitochondrial membrane potential and inhibiting ROS formation of substantia nigra dopaminergic neurons. *Biochim Biophys Acta - Mol Basis Dis*. 2011;1812(6):674–684. doi:10.1016/j.bbadis.2011.03.007
53. Gvozdjáková A, de Cabo R, Navas P. Mitochondrial medicine. *Recent Adv Mitochondrial Med Coenzyme Q*. 2018;1–11. doi:10.1161/circulationaha.108.775163
54. Zorova L, Popkov V, Plotnikov E, et al. Mitochondrial membrane potential Ljubava. *Anal Biochem*. 2018;552:50–59. doi:10.1016/j.ab.2017.07.009